Agricultural Systems 161 (2018) 16–27

Contents lists available at ScienceDirect

Agricultural Systems

journal homepage: www.elsevier.com/locate/agsy

Contributions of climate change to the boundary shifts in the farming-pastoral ecotone in northern China since 1970

Wenjiao Shi[a,b,c,*], Yiting Liu[a,c], Xiaoli Shi[d,e,**]

[a] Key Laboratory of Land Surface Pattern and Simulation, Institute of Geographic Sciences and Natural Resources Research, Chinese Academy of Sciences, Beijing 100101, China
[b] Key Laboratory of Carrying Capacity Assessment for Resource and Environment, Ministry of Land and Resources, Beijing 101149, China
[c] College of Resources and Environment, University of Chinese Academy of Sciences, Beijing 100049, China
[d] College of Resources and Environment Sciences, Hebei Normal University, Shijiazhuang 050024, China
[e] Key Laboratory of Environmental Evolvement and Ecological Construction of Hebei Province, Shijiazhuang 050024, China

ARTICLE INFO

Keywords:
Contributions
Boundary shift
Farming-pastoral ecotone
Climate change
Land use

ABSTRACT

Critical transitions of farming-pastoral ecotone (FPE) boundaries can be affected by climate change and human activities, yet current studies have not adequately analyzed the spatially explicit contributions of climate change to FPE boundary shifts, particularly those in different regions and periods. In this study, we present a series of analyses at the point (gravity center analysis), line (boundary shifts detected using two methods) and area (spatial analysis) levels to quantify climate contributions. This was done at a 1-km scale in each ecological functional region during three study periods from the 1970s to the 2000s using climate and land use data. Both gravity center analysis and boundary shift detection revealed similar spatial patterns with more extensive boundary shifts in the northeastern and southeastern parts of the FPE in northern China, especially during the 1970s–1980s and 1990s–2000s. Climate contributions in the X- and Y-coordinate directions and in the directions of transects along boundaries showed that significant differences in climate contributions to FPE boundary shifts existed in different ecological functional regions during the three periods. Additionally, the results in different directions exhibited good agreement in most of the ecological functional regions during most of the periods. However, the values of contributions in the directions of transects along the boundaries (1–17%) were always smaller than those in the X-and Y-coordinate directions (4–56%), which suggests that the analysis in the transect directions is more stable and reliable. Thus, this is an alternative method for detecting the climate contributions to boundary shifts associated with land use changes. Spatial analysis of the relationship between climate change and land use change in the context of FPE boundary shifts in northern China provides further evidence for explanation of the driving forces of climate change. Our findings provide an improved understanding of the quantitative contributions of climate change to the formation and transition of FPE in northern China, which will be essential for addressing current and future adaptation and mitigation measures and regional land use management.

1. Introduction

The land use change in an ecotone is a major concern for fragile ecosystem management (Van Vliet et al., 2012). In future decades, climate changes and human activities are expected to produce large shifts in land use/cover distributions at unprecedented rates, which are expected to be the most rapid and extreme at the ecotone level (Allen and Breshears, 1998; IPCC, 2013; Pricope, Husak, Lopez-Carr, Funk, and Michaelsen, 2013). The farming-pastoral ecotone (FPE) is particularly sensitive to climate change (Allen and Breshears, 1998; Blanco et al., 2014; Fu, 1992; Silva, 2014; Wasson, Woolfolk, and Fresquez, 2013). Therefore, it has been suggested that FPE boundary shifts be considered the prominent indicators for the impacts of climate change because interactions between various ecosystems will often occur at these boundaries (Berner, Beck, Bunn, and Goetz, 2013; Hansen, Di Castri, and Naiman, 1988; Kitzberger, 2012; Scheffer, Hirota, Holmgren, Van Nes, and Chapin, 2012; Sharma, Vetaas, Chaudhary, and Måren, 2014; Williams et al., 2013). Because of the

* Correspondence to: W. Shi, Institute of Geographic Sciences and Natural Resources Research, Chinese Academy of Sciences. 11A, Datun Road, Chaoyang District, Beijing 100101, China.
** Correspondence to: X. Shi, College of Resources and Environment Sciences, Hebei Normal University, No.20 Road East. 2nd Ring South, Yuhua District, Shijiazhuang 050024, China.
E-mail addresses: shiwj@lreis.ac.cn (W. Shi), shixiaoli_2004@163.com (X. Shi).

https://doi.org/10.1016/j.agsy.2017.12.002
Received 22 January 2017; Received in revised form 30 November 2017; Accepted 3 December 2017
Available online 08 December 2017
0308-521X/

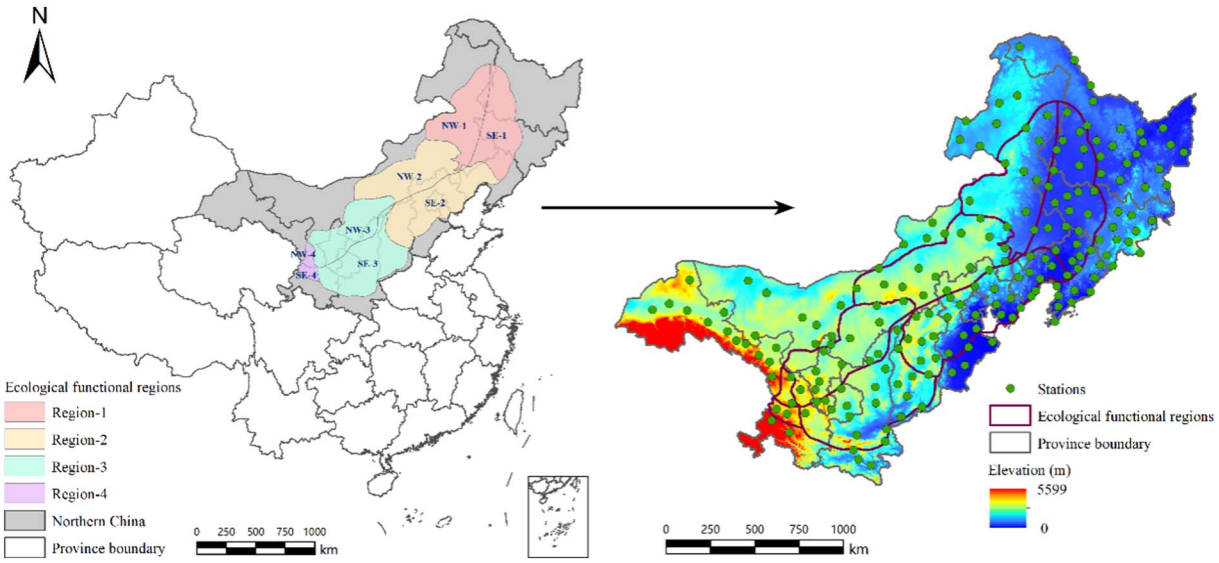

Fig. 1. The location of the FPE in northern China (left) and the distribution of meteorological stations and elevation (right).

large area and range, extraordinarily fragile environment and natural climate variability of the FPE in northern China, it has been the focus of investigations of the response of an ecosystem to climate change (Chen, Huang, and Wang, 2015; Fu, Qi, and Chang, 2015; Wang, Jiang, Liao, and Deng, 2015; Wu, Zhan, Yan, Shi, and Huang, 2013; Yu et al., 2014).

In recent decades, an increasing number of researchers have documented the relationship between boundary shifts and historical climate change in the FPE of northern China (Fang, Ye, and Zeng, 2007; Ge et al., 2015; Ge, Liu, Zheng, and Xiao, 2013; Ye and Fang, 2012; Ye, Fang, and Khan, 2012; Ye, Fang, Ren, Zhang, and Chen, 2009). From 1500 BCE to the 4th century BC, the cold and dry climate caused a southward shift of the FPE by 2–5° latitude (Han, 2000). From the late Qin to the West Han Dynasty (221 BCE–50 BCE) periods in Chinese history, the northern boundary of the FPE moved northward from 39°N to 41°N corresponding to a comparatively warm climate in East and Central China (Ge et al., 2013). Moreover, Fang et al. (2007) found that the cropland boundary changes in Northeast China from 1661 to 1680 were due to the drought events that occurred in North China. Since the mid-19th century, the rapid expansion of the northern FPE boundary has benefited from a warming climate (Ye et al., 2012). Although most previous studies did not separate the combined effects of climate change and human activities, some of the semi-quantitative relationships between boundary shifts and climate change were analyzed. In these studies, boundary shifts were closely related to historical climate change, and boundaries moved northward in accordance with wetter and warmer climate conditions, and vice versa. However, the quantitative contributions of climate change to boundary changes in different ecological regions of the FPE in northern China have not been evaluated.

Some studies analyzed the relationship between boundary shifts and modern climate change in different regions of the FPE, but inconsistent conclusions were yielded. Liu, Gao, Lv, Han, and Nie (2011) found that the land use boundary of FPE had moved northwest due to climate change in recent decades, whereas Lu and Jia (2013) concluded that the fluctuations in the FPE boundary were closely related to precipitation variations. One of our recent studies illustrated the relationship between climate and cropland changes in northern China based on a spatial grid (Shi et al., 2014), but it did not focus on the specific contributions of climate change to the boundary shifts in different regions and periods.

The FPE is a transition zone between sub-humid region and arid/semi-arid region. This is a very sensitive and vulnerable region, so human adaptation or management measures should be highly related to the climate contributions. Although some insight is available regarding the effects of climate change on FPE boundary shifts, our understanding of the spatially explicit contributions of climate change at 1-km scale remains limited. Understanding climate contributions in different regions and periods is essential for generating knowledge required to make reasonable decisions concerning human adaptability to climate change in different spatial regions. For the regions with significant contributions of climate change, decision makers can alter crop or pasture varieties, alter sowing date, and improve infrastructural investment to adapt to the changing heat or water conditions due to climate change, so the advantages of climate change can be utilized and disadvantages can be avoided.

Here, we present a complete analysis framework at the point, line and area levels in order to quantify the spatially explicit climate contributions and to detect the driving forces at a 1-km scale to investigate the FPE boundary shifts in northern China in response to climate change from the 1970s to the 2000s. It is the first attempt at systematically quantifying the contributions of climate change to FPE boundary shifts in northern China. The objectives of our study were as follows: i) to describe the boundary changes of the FPE based on land use and climate change from the 1970s to the 2000s; ii) to explore the different spatiotemporal patterns of FPE boundary shifts in northern China associated with climate changes; and iii) to analyze the driving forces of climate change for the FPE boundary shifts at a 1-km grid scale during the study period.

2. Materials and methods

2.1. Study area

The study area (31°43′–53°34′N and 92°20′–135°05′E) is a transitional zone between arid and semi-arid pastoral grasslands to the northwest and traditional intensive cropland to the southeast (Liu et al., 2011). This zone covers areas of ten provinces, autonomous regions or metropolises: Heilongjiang, Jilin, Liaoning, Inner Mongolia, Hebei, Beijing, Shanxi, Shaanxi, Ningxia and Gansu (Fig. 1). The mean annual temperature in this area is 2–8 °C, and the mean annual precipitation varies from 300 mm in the northwest to 500 mm in the southeast. In the past 40 years, most of the area has suffered from increasingly warming temperatures and frequent drought (Shi et al., 2014; Wang et al., 2015), and cropland areas have been influenced by climate change (Shi et al., 2014). Meanwhile, human activities, such as overgrazing and land use policies, have seriously disturbed the boundary of the FPE. Thus, the

boundary of the FPE in northern China has changed as a result of complex and dynamic interactions between climate change and human activities (Gyasi et al., 1995; Staver, Archibald, and Levin, 2011; Wang et al., 2015).

To identify the climate contributions to FPE boundary fluctuations in different regions, the study area can be divided into eight ecological functional regions according to their ecosystem services and geographical locations (Huang, Xin, and Zhang, 2010): the northwest (NW-1) and the southeast (SE-1) cropland areas on the southeastern fringe of the Greater Hinggan Mountains, the northwest (NW-2) and southeast (SE-2) agricultural-forestry-pastoral production regions on the southeast fringe of the Inner Mongolian Plateau, the northwest (NW-3) and the southeast (SE-3) farming-pastoral regions on the northern Loess Plateau, and the northwest (NW-4) and southeast (SE-4) arid desert-oasis cultivated regions in the Hexi Corridor (Fig. 1). The division line between the northwest and southeast was the 400 mm average isohyet from the 1970s to the 2000s.

2.2. Data

2.2.1. Climate data

Climate data in the study area were collected at 197 meteorological stations from 1971 to 2010 and obtained from the National Meteorological Center of the China Meteorological Administration (Fig. 1). After bias adjustment based on the observation time, instrument changes and station movement, the Multiple Analysis of Series for Homogenization (MASH) software package was used to create a dataset of the study area consisting of the homogenized daily mean temperature series (Li and Yan, 2009). Additionally, daily precipitation data were retrieved from the Data and Information Center of the China Meteorological Administration. The active accumulated temperatures ≥ 10 °C (AAT10), the standardized precipitation evapotranspiration index (*SPE*I) and the trends of these two indices at each national meteorological station in northern China in the 1970s–1980s, 1980s–1990s and 1990s–2000s were calculated, and the methods were described in detail in our previous study (Shi et al., 2014).

2.2.2. Land use data

The focus of our study was an ecotone located between cropland and grassland in northern China. Cropland and grassland data in the 1970s (1972–1979), 1980s (1987–1990), 1990s (1999–2000) and 2000s (2008–2010), cropland and grassland change data from the 1970s to 1980s, the 1980s to 1990s and the 1990s to 2000s were obtained from the National Land Use/Land Cover datasets (NLCD), generated in the second nationwide land cover and land use classification project (Liu et al., 2005; Liu, Liu, Zhuang, Zhang, and Deng, 2003; Liu et al., 2010). These data were derived through the visual interpretation of images from Landsat TM/ETM/MSS, and supplemented with CBERS-1 and CBERS-2 images. Area percentages of land use types in each 1 km^2 grid were converted from vector data using the methods proposed in previous studies and used for the delineation of FPE boundaries during different periods (Liu et al., 2005; Liu et al., 2003; Liu et al., 2010). The validation and accuracy of these data were assessed in detail in previous studies (Shi et al., 2014; Zhang, Zhao, and Wang, 2012).

2.3. The analysis framework at the point, line and area levels to quantify climate contributions

We present a complete analysis framework at the point, line and area levels to quantify the spatially explicit climate contributions at the 1-km scale and detect the driving forces of the FPE boundary shifts (Fig. 2). First, we delineated the FPE boundaries and detected the boundary shifts based on the climate and land use data in different periods from the 1970s to the 2000s using gravity center analysis at the point level, and using two methods at line level to detect the shifts in the X- and Y-coordinate directions and in the directions of transects along boundaries. The climate boundary of FPE is controlled only by climate condition, which can be regarded as the boundary generated that was based on climate conditions without any influence of human factors, whereas land use boundary of the FPE is the realistic boundary which is affected by both climate change and human activities. Thus, the response of the FPE boundary based on land use data to climate change can be determined by quantifying the changes in the FPE boundary based on climate and land use data. Based on the relationship between the shift distances of climate boundary and land use boundary, we identified the effects of climate change and human activities on the FPE boundary shifts in different ecological functional regions during the three periods. Finally, spatial analysis of driving forces of climate change in land use change regions was conducted at area level in the spatio-temporal change area based on the changes of the AAT10 and *SPE*I.

2.3.1. Delineation of FPE boundaries based on both climate and land use data

To determine the effects of climate on FPE boundary shifts, we delineated the FPE boundaries in northern China based on both climate and land use data. The criteria for the delineation of FPE boundaries were given in detail in Shi, Liu, and Shi (2017).

First, the FPE boundary based on climate data was defined according to the following conditions: (i) the 400 mm isohyet is located in the center of the FPE; (ii) the 500 mm and 300 mm isohyets are used to identify the southeastern and northwestern boundaries of FPE, respectively; and (iii) the FPE boundary is defined based on an aridity index of 0.2–0.5 and precipitation variability of 15–30%, as recommended by Liu et al. (2011).

Second, the FPE boundary based on land use data should satisfy the following conditions: (i) the area percentages of both cropland and grassland in a 1 km × 1 km grid should be > 15% (Wang and Shi, 1988; Ye and Fang, 2012) and (ii) the total area percentages of cropland and grassland in a 1 km × 1 km grid are generally > 50% (Wu and Guo, 1994). The boundaries were manually digitized in ArcGIS 10.3 according to these conditions.

2.3.2. The detection of FPE boundary changes in different periods

2.3.2.1. Gravity center shifts of the FPE. Gravity center analysis can identify the directions and distances of shifts associated with land use and land cover changes during the study periods, and it has been applied in geography since the 1950s (Ebdon, 1985; Hart, 1954). Finding the gravity center is an effective way of pinpointing the geometric center of a specified region. In each period, the gravity center of each ecological functional region was produced using the feature-to-point function in ArcGIS 10.3 (Fernández, Hamilton, and Kueppers, 2015; Zuo et al., 2014). Based on the latitude and longitude coordinates of the gravity centers, the directions and distances of gravity center shifts in different periods were calculated by Euclidean distance transformation.

2.3.2.2. FPE boundary shifts of coordinates in the X- and Y-directions. The FPE boundary shifts of coordinates in the X- and Y-directions can be calculated according to the overlay of a 1 km × 1 km fishnet generated in the ecological functional region (Fig. 3a). A number of lines with a 1-km interval in the X- (the sequence number of the lines named as MarkID increases from south to north, MarkID: i, $i + 1$, $i + 2$…) and Y-directions (MarkID increases from west to east, MarkID: j, $j + 1$, $j + 2$…) can be achieved (Fig. 3a). The fishnet lines overlaid the four periods of FPE boundaries during the 1970s, 1980s, 1990s and 2000s, and four intersection points were achieved for each line (Fig. 3a, I and II). Thus we can calculate the distances from the former period (*fp*) to the latter period (*lp*) in each line i overlaid with land use (LU_{ifp_lp}) and climate boundaries (C_{ifp_lp}). Because the sequences of fishnet lines overlaid the boundaries during different periods were related with

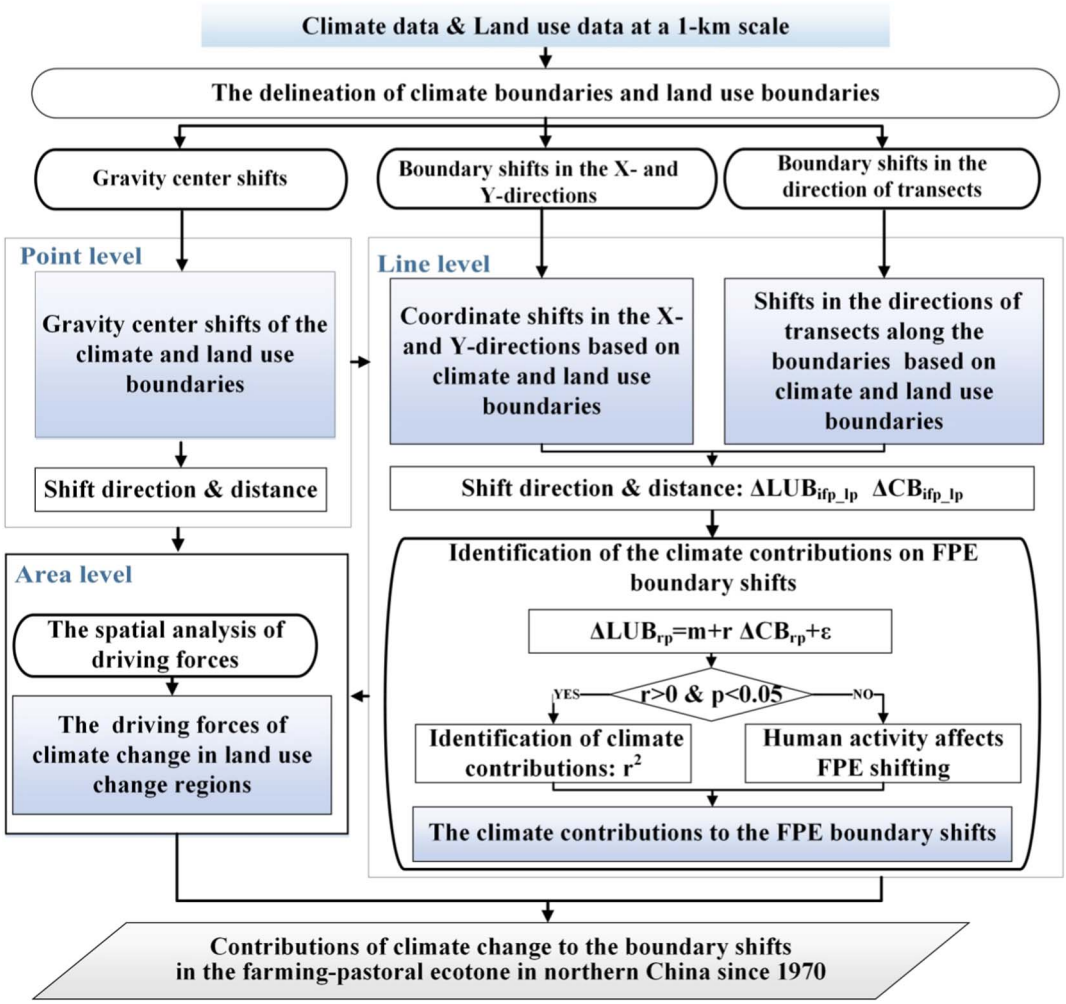

Fig. 2. The framework for the analysis of the climate contributions to the boundary shifts in the FPE.

the boundary shift directions, we recorded the direction (*Direction*) of the distance from the former (latter) period to the latter (former) periods as 1 (−1), indicating that the boundary moved eastward (westward) or northward (southward) (Fig. 3a, I and II); if the fishnet line crossed the boundary during the same period, the direction was recorded as 0. Thus the shifts of climate (ΔLUB_{ifp_lp}) and land use boundaries (ΔCB_{ifp_lp}) during different periods were extracted at coordinates in the X- and Y-directions in each fishnet line *i*,

$$\Delta LUB_{ifp,lp} = LU_{ifp,lp} \times Direction \quad (1)$$

$$\Delta CB_{ifp,lp} = C_{ifp,lp} \times Direction \quad (2)$$

where *fp* is the former period, and *lp* is the latter period; ΔLUB_{ifp_lp} and ΔCB_{ifp_lp} are the distances with shift directions based on the land use boundaries and climate boundaries changed during different periods at fishnet line *i*; LU_{ifp_lp} and C_{ifp_lp} are the distances based on the land use boundaries and climate boundaries changed during different periods at fishnet line *i*.

The distances and directions of the changes were calculated in each grid of the fishnet according to the Eqs. (1) and (2); thus, the boundary shifts at coordinates in the X- and Y-directions in the 1970s–1980s, 1980s–1990s and 1990s–2000s in different ecological functional regions were detected (Shi et al., 2017).

2.3.2.3. The FPE boundary shifts in the direction of transects along the boundaries. The Digital Shoreline Analysis System (DSAS), provided by the U.S. Geological Survey, is often used to compute shoreline changes from a time series of multiple shoreline positions (Adnan, Hamylton, and Woodroffe, 2016; Jayson-Quashigah, Addo, and Kodzo, 2013; Kallepalli, Kakani, James, and Richardson, 2017; Thieler, Himmelstoss, Zichichi, and Ergul, 2009). We used DSAS to calculate the FPE boundary shifts in the direction of transects along the boundaries. To guarantee that each baseline segment had all boundaries on one side, we digitized baselines manually after buffering the existing boundaries (Fig. 3b). From the start of the baseline (TransectID = 0), transects were generated at a spacing of 1 km along the baseline using the smoothed baseline cast method (Fig. 3b). The transects crossed the land use and climate boundaries during the four periods, so the intersection points between the transects and the boundaries during different periods were achieved. Distances of boundary shifts from the interaction of transect *i* crossed to the land use and climate boundaries (LU_{ip} or C_{ip}) can be calculated according to the Eqs. (3) and (4),

$$\Delta LUB_{ifp,lp} = LU_{ilp} - LU_{ifp} \quad (3)$$

$$\Delta CB_{ifp,lp} = C_{ilp} - C_{ifp} \quad (4)$$

where ΔLUB_{ifp_lp} and ΔCB_{ifp_lp} are the distances of land use and climate boundary shifts in the transect *i*; LU_{ifp} (LU_{ilp}) and C_{ifp} (C_{ilp}) are the distances from land use and climate boundaries to the baseline during the former (latter) periods, respectively.

The net boundary movement of the distance between the former and latter boundaries of the FPE at each transect can be determined to measure boundary shifts in the direction of transects along the

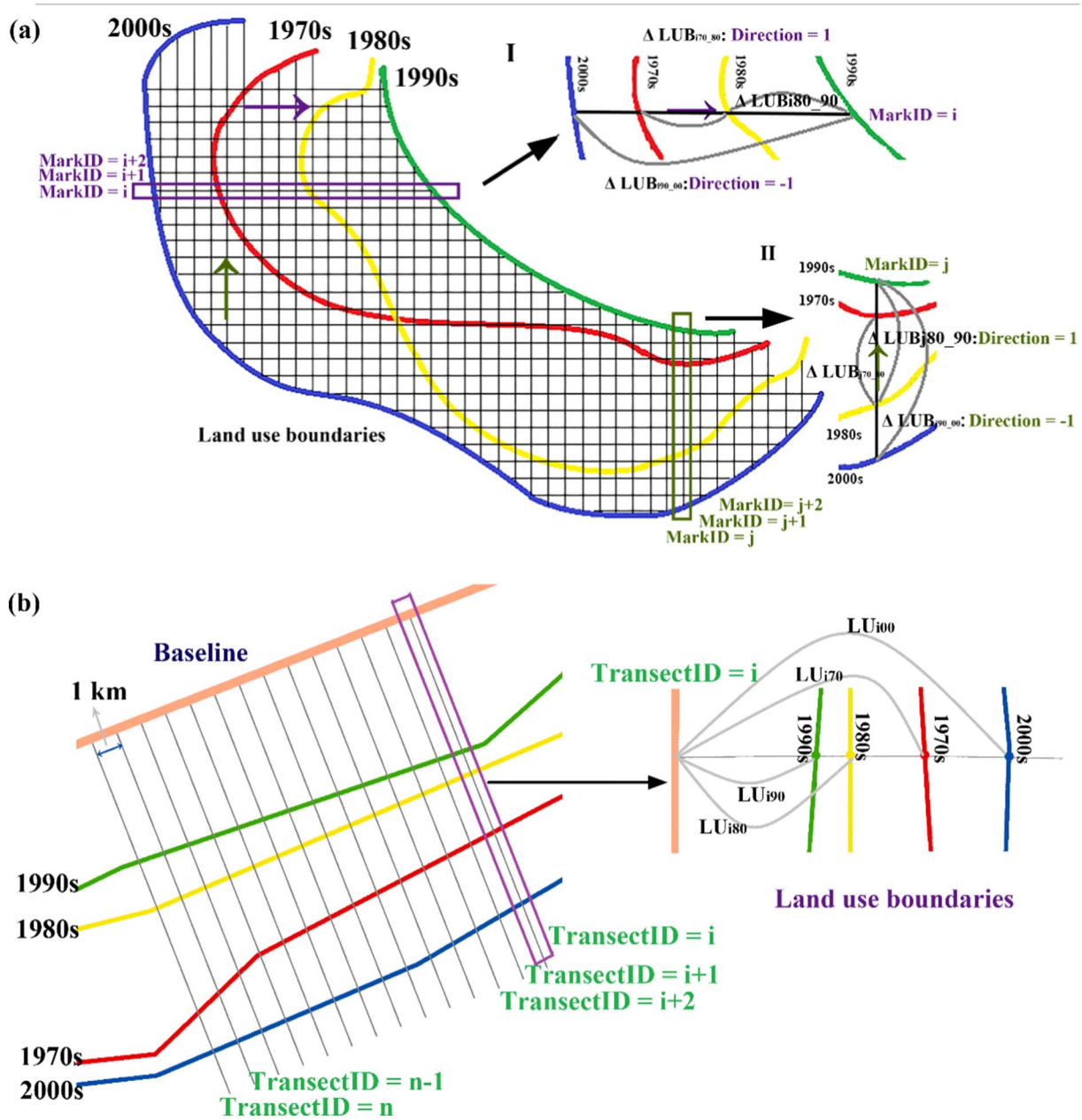

Fig. 3. Diagram of the FPE boundary shifts detected (a) at coordinates in the X- and Y-directions and (b) in the direction of transects along the boundaries. ΔLUB_{i70_80} (ΔCB_{i70_80}): the distance from the intersection point of fishnet i and the land use (climate) boundary in the 1970s to the intersection point of fishnet and the land use (climate) boundary in the 1980s. The meanings of ΔLUB_{i80_90} (Δ CB_{i80_90}) and ΔLUB_{i90_00} (Δ CB_{i90_00}) are similar to ΔLUB_{i70_80} (ΔCB_{i70_80}). $LU_{i70}(C_{i70})$: the distance from the baseline to the intersection point of transect i and the land use (climate) boundary in the 1970s. The meanings of LU_{i80} (C_{i80}), LU_{i90} (C_{i90}) and LU_{i00} (C_{i00}) are similar to $LU_{i70}(C_{i70})$.

boundaries during the 1970s–1980s, 1980s–1990s, and 1990s–2000s (Shi et al., 2017).

2.3.3. Identification of the climate contributions on FPE boundary shifts

To assess the impacts of climate change on the FPE boundary shifts, we explored the relationship between climate boundary shifts and land use boundary shifts by analyzing changes in the X- and Y-coordinate directions and in the directions of transects along the boundaries in the 1970s–1980s, 1980s–1990s, and 1990s–2000s.

To detect the effects of climate change on FPE boundary shifts, we conducted a correlation analysis using 24 subsets of boundary shift data based on climate and land use data in each fishnet grid (1 km × 1 km) or along each transect (1 km). The 24 subsets included data from the two parts of the four ecological functional regions (Fig. 1: NW-1 to NW-4 and SE-1 to SE-4) during the three study periods (1970s–1980s, 1980s–1990s, and 1990s–2000s). If the correlation analysis shows that the positive correlation is significant between climate and land use boundary shifts in a given region during a given period, the climate change is considered to have significant contribution to the FPE boundary shifts (land use boundary shifts). We used the statistical significance of the positive correlations to determine the contributions. We then applied a linear model to the datasets of boundary shifts based on climate and land use data in fishnet grids or along transects in both parts of the four regions:

$$\Delta LUB_i = m + r\Delta CB_i + \varepsilon \quad (5)$$

where ΔLUB_i is the observed shift distance of the land use boundary in fishnet grid i (in the X- and Y-coordinate directions) or along transect i (in the direction of transects along the boundaries); m is the FPE boundary change due to human factors, such as cost, price, demand,

and agricultural or livestock products and policies; ΔCB_i is the climate boundary shift in fishnet grid i or along transect i; r is the response of the boundary shift based on land use data to climate change; and ε is the residual error. If r is > 0 and p is lower than 0.05, climate change has significant effects on the FPE boundaries; otherwise climate change has no significant effects. The climate contributions to land use boundary of the FPE in northern China were reflected by the squared correlation coefficients of the significant positive correlations (Lobell and Asner, 2003; Shi et al., 2017).

2.3.4. The spatial analysis of driving forces of climate change in land use change regions

To determine the driving forces of climate change in land use change regions, we further selected the cropland change or grassland change regions in the FPE of northern China and analyzed the effects of climate change on land use change at a 1-km grid scale in these regions. The AAT10 and *SPE*I changes in the cropland change or grassland change regions were quantitatively compared using the raster calculation and zonal statistics tools in ArcGIS 10.3. The changes in AAT10 (or *SPE*I) in each grid in the 1970s–1980s, 1980s–1990s and 1990s–2000s were calculated by subtracting AAT10 (or *SPE*I) in the latter period from that in the prior period (Shi et al., 2014).

3. Results and discussion

3.1. Shifts in the FPE boundary based on the climate in northern China

3.1.1. Gravity center shifts

The gravity center analysis based on climate boundaries showed that there were large differences in the boundary shifts in different ecological functional regions during the 1970s–1980s, 1980s–1990s and 1990s–2000s (Fig. 4a). In the two parts (NW and SE) of four regions (regions 1–4) in FPE, the average ranges of gravity center shifts during the three periods decreased from Northeast China (region 1, 63.2 km) to Northwest China (region 4, 12.1 km), and those in the southeast (SE, 54.0 km) were significantly larger than those in the northwest (NW, 24.3 km) in the three periods. The gravity centers in region 1, NW-3 and SE-2 moved southwestward during the 1970s–1980s. Then, the boundaries in those regions shifted to the northeast. However, the changes in direction of the gravity centers were different in NW-2, SE-3 and region 4 during different periods. An average shift of 51.2 km was the most extensive, which occurred during the 1970s–1980s, and an average shift of 39.4 km during the 1990s–2000s was the second. Region 1 experienced the largest shift in the 1970s–1980s, with a southwestward move of 138.1 km in the SE part and a 97.8 km in the NW part.

3.1.2. Coordinates shifts in the X- and Y-directions

The spatial patterns observed in the gravity center analysis were further illustrated by the FPE boundary shifts of coordinates in the X- and Y-directions, which showed that greater shifts took place in regions 1 and 2, followed by those in regions 3 and 4 during the three periods. Similar to the results of gravity center changes, the boundary shifts in most of the regions in the X direction showed a westward move during the 1970s–1980s. Then they moved eastward in regions 3, 4 and SE-1 during the 1980s–1990s. Most of the regions moved eastward during the 1990s–2000s except for region 3 and NW-4. Meanwhile, the detection in the Y-coordinate direction showed that the boundary shifts in region 1, NW-3 and SE-2 shifted to the south significantly during the 1970s–1980s. The largest shifts were observed in NW-1 with an average distance of 128.27 km, and moved to the north in this region. In the X-coordinate direction, the largest shift distances of 278.5 km and 238.8 km were observed in SE-2 during the 1990s–2000s and in NW-1 during the 1970s–1980s (Fig. 4b). In the Y-coordinate direction, the most extensive shifts of 271.3 km and 235.4 km occurred in NW-1 and SE-1 during the 1970s–1980s (Fig. 4c).

3.1.3. Shifts in the directions of transects along the boundaries

We provided the averages and ranges of climate boundary shifts in the transect directions along the boundaries of the NW and SE parts in different ecological functional regions, as shown in Fig. 4d. Similar to the results of coordinate shifts in the X- and Y-directions, great fluctuations were observed in the FPE of region 1 (NW-1 and SE-1) and region 2 (NW-2 and SE-2) in northern China. The climate boundary moved southward significantly in region 1, NW-3 and SE-2 during the 1970s–1980s, and the intense shifts of > 270 km occurred in both NW-1 and SE-1 during this period. The shift ranges decreased in both NW-1 and SE-1 after the 1980s, except from 1990s–2000s in NW-1.

3.2. Shifts in the FPE boundary based on land use in northern China

3.2.1. Gravity center shifts

The gravity center analysis, based on the land use boundary of the FPE in northern China (Fig. 5a), yielded trends that were similar to those based on climate change (Fig. 4a). The average shift distances during the three periods were 17.3 km and 15.8 km in regions 1 and 2, respectively, which were greater than those in regions 3 (6.0 km) and 4 (3.4 km). Additionally, the average shift in the gravity center based on land use data in the SE part (14.0 km) was more extensive than that in the NW part (7.3 km). The land use boundaries exhibited intense shifts during the 1970s–1980s (average shift of 11.4 km) and 1990s–2000s (average shift of 11.8 km), and those based on climate were similar, especially in the NW parts of regions 1 and 2. The greatest change emerged in SE-2 in the 1990s–2000s, the boundary moving 42.7 km southwestward. During the 1970s–1980s, land use boundaries in most of the regions moved eastward except for NW-4, while they moved in the opposite direction except for SE-2 during the 1980s–1990s. Although gravity center shifts in most of the regions moved in different directions during the 1990s–2000s, region 1 and NW-3 both moved to the northeast.

3.2.2. Coordinate shifts in the X- and Y-directions

The shifts based on land use boundaries of coordinates in the X- and Y-directions were less than half as extensive as those based on climate. The shifts in regions 1 and 2 were greater than those in the other regions. The most extensive shift of 140.4 km was observed in SE-2 in the 1970s–1980s in the X-coordinate direction, and the largest average distance of 103.3 km was observed in NW-1 during the 1980s–1990s (Fig. 5b). In the Y-coordinate direction, the most extensive shift of 149.8 km moving northward occurred in NW-2 during the 1970s–1980s, and the largest shift of 125.7 km moving northward was also observed in SE-1 during the 1990s–2000s (Fig. 5c).

Similar to the detection results of gravity center shifts, the boundary shifts in most of the regions (except for NW-2) in the X-coordinate direction moved eastward during the 1970s–1980s, while the boundaries shifted westward during the 1980s–1990s. The directions of boundary shifts were different during the 1990s–2000s. In the Y-coordinate direction, the directions of boundary shifts varied during the 1970s–1980s, and moved northward during the 1980s–1990s except for SE-1 and SE-3. During the 1990s–2000s, boundaries in most regions moved southward except for region 1. Boundary shifts moved northward in region 1 with the largest average ranges (28.3 km in NW-1 and 50.6 km in SE-1) during this period.

3.2.3. Shifts in the directions of transects along the boundaries

Shifts in the directions of transects along the boundaries showed that the average distance of shifts was most extensive in region 1 (25.4 km), followed by those in region 2 (11.9 km), region 3 (9.2 km) and region 4 (4.4 km) (Fig. 5d). Similar to the shifts based on climate, the greatest fluctuations occurred in SE-1 (163.3–217.8 km) and NW-1 (135.5–182.8 km) during the three periods, followed by those in NW-2 (53.2–91.6 km) and SE-2 (48.2–80.0 km).

Similar to the detection in the X- and Y- coordinate directions, most

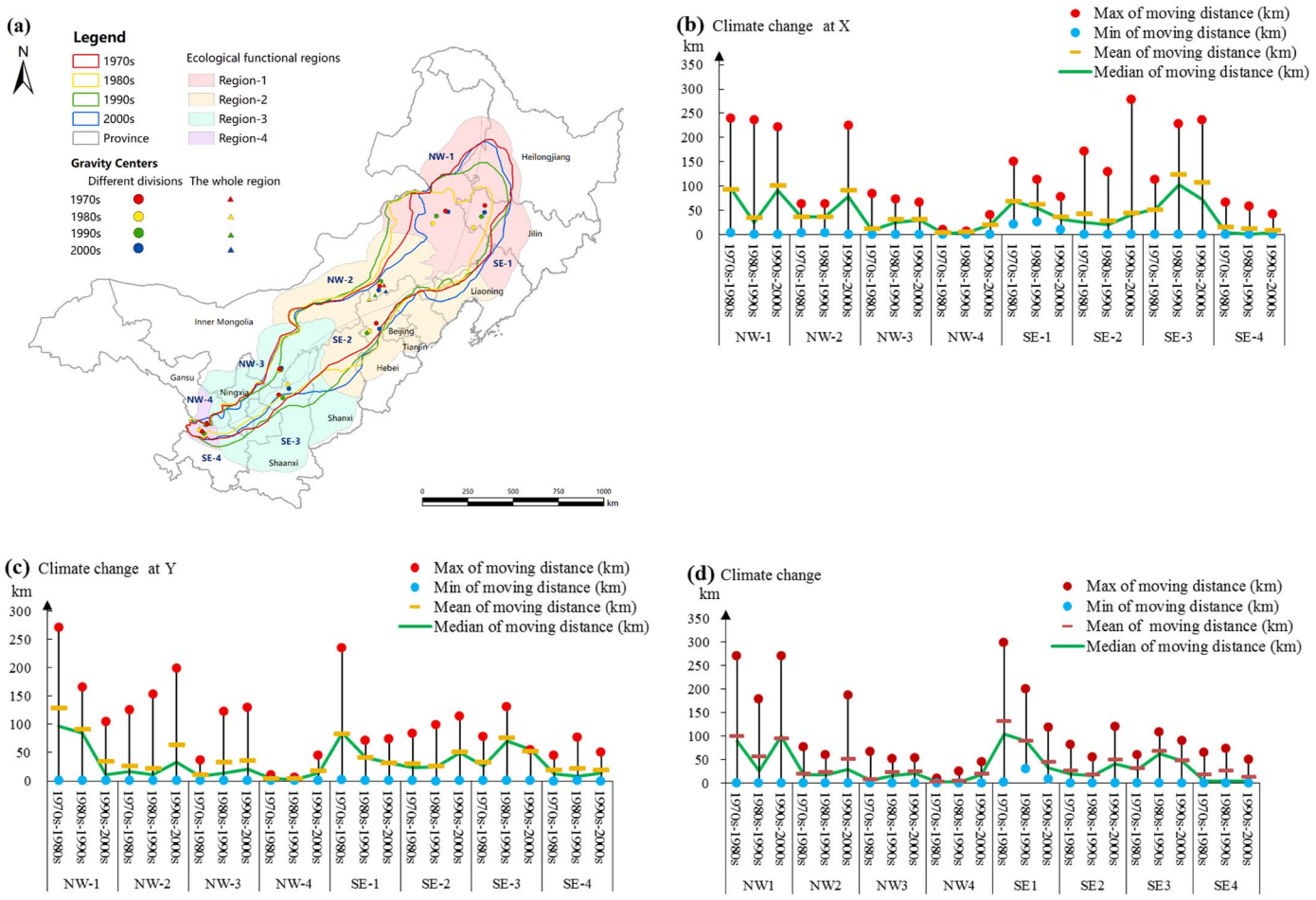

Fig. 4. The spatial distributions of FPE boundary shifts based on climate change in each ecological functional region during the 1970s–1980s, 1980s–1990s and 1990s–2000s: (a) gravity center and (b) distances of changes in the X-coordinate direction, (c) Y-coordinate direction and (d) transect directions along boundaries.

of the boundaries moved southward during the1970s–1980s, and then moved northwestward except for SE-1 during the 1980s–1990s. During the 1990s–2000s, the largest average shift distance was observed in region 1 (27.4 km in NW-1 and 22.4 km in SE-1).

3.3. Climate contributions to the FPE boundary shifts

3.3.1. Climate contributions of coordinates in the X- and Y-directions

In the X-coordinate direction of region 1, the FPE boundaries based on both climate and land use have extended westward simultaneously due to the warm and dry climate in NW-1 since the 1970s (Fig. 6). Climate contributions to the FPE boundary shifts in NW-1 in the X-coordinate direction were 44%, 11% and 20% during the 1970s–1980s (Fig. 6a), 1980s–1990s (Fig. 6b) and 1990s–2000s (Fig. 6c), respectively. By contrast, in the Y-coordinate direction of NW-1, the correlation was not significant during the former two periods. The FPE boundary based on climate change in SE-1 was less sensitive to temperature than to precipitation, while the northward shift of the FPE boundary in NW part of the region based on land use can be attributed to climate warming.

In the X-coordinate direction in region 2, the FPE boundaries based on climate and land use in NW-2 mainly shifted westward during the 1970s–1980s (Fig. 6a), and those in SE-2 exhibited similar trends during the 1980s–1990s (Fig. 6b). The climate contributions to the FPE boundaries in these two regions during these periods were 21% and 4%. In the Y-coordinate direction, climate change significantly affected the FPE boundaries in NW-2, with various shift directions during the three periods. The FPE boundaries shifted northward in the former two periods and southward beginning in 2000. The climate contributions to the FPE boundaries in NW-2 were 9%, 56% and 10% during the 1970s–1980s, 1980s–1990s and 1990s–2000s, respectively.

The effects of climate change on the FPE boundary shifts were less significant in regions 3 and 4 than the other two regions, indicating that the FPE boundary shifts in the west of the FPE were mainly affected by human activities. In the X-coordinate direction in region 3, the FPE boundaries based on climate and land use moved westward only in the southeastern part (SE-3) in the 1970s–1980s, with 20% of the shift associated with climate change. In the Y-coordinate direction, 8% and 23% of the FPE boundaries in NW-3 during the 1980s–1990s and SE-3 during the 1970s–1980s, respectively, were affected by climate change.

3.3.2. The climate contributions in the directions of transects along the boundaries

The climate contributions to the FPE boundary shifts in the transect direction were similar to those in the X- and Y-coordinate directions (Fig. 7). In region 1, climate change caused the FPE boundaries to shift northward after 2000 in both the northwest (NW-1) and southeast (SE-1), with contributions of 1% and 2% ($p < 0.01$), respectively (Fig. 7c). In region 2, a climate contribution of 17% ($p < 0.01$) to a northwestward shift in the FPE boundary during the 1970s–1980s was detected in the northwest (NW-2) (Fig. 7a), and the FPE boundary shifted to the southeast due to a 4% ($p < 0.01$) contribution during the 1990s–2000s (Fig. 7c). In the southeastern part of the region (SE-2), the FPE boundary moved northwestward, and the climate contribution was 3% ($p < 0.01$) during the 1980s–1990s (Fig. 7b). The boundaries in the southeastern part of region 3 (SE-3) moved northwestward due to a

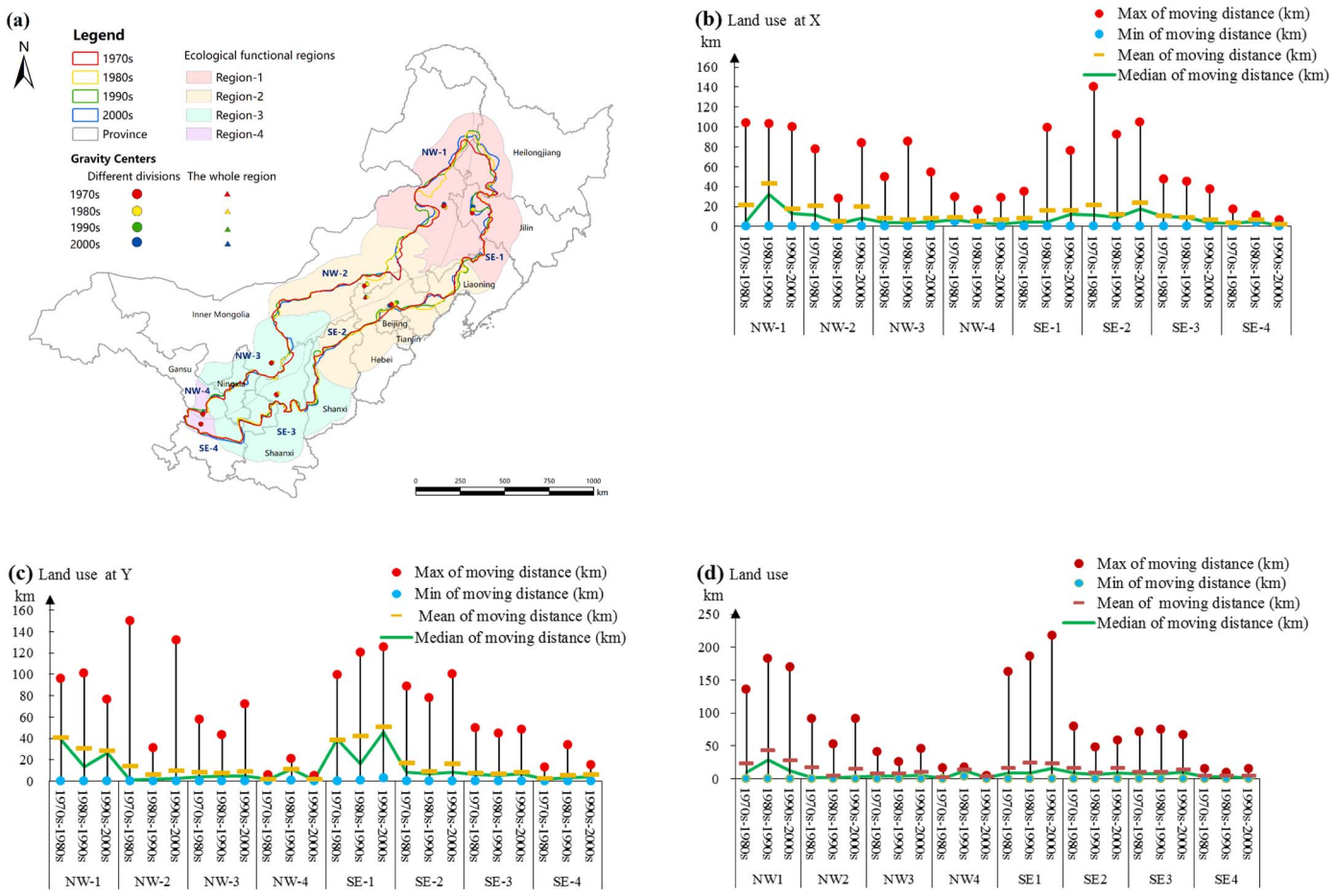

Fig. 5. The spatial distributions of FPE boundary shifts based on land use in each ecological functional region during the 1970s–1980s, 1980s–1990s and 1990s–2000s: (a) gravity center and (b) distances of changes in the X-coordinate direction, (c) Y-coordinate direction and (d) transect directions along boundaries.

10% ($p < 0.01$) climate contribution, and those in the northwestern part of region 4 (NW-4) moved southeastward as a result of a 15% ($p < 0.01$) climate contribution during this period (Fig. 7a). From the 1980s–1990s, the boundary in NW-3 exhibited a northwestward shift, and the climate contribution was 4% ($p < 0.01$) (Fig. 7b). During the 1990s–2000s, the climate contribution to the boundary shift in SE-3 was 2% ($p < 0.01$) (Fig. 6c).

3.4. Spatial analysis of the driving forces of climate change in land use change regions

Climate warming or wetting is helpful for the reclamation of cropland, which resulted in the shifts of FPE boundaries during the three periods. For example, climate warming led to the cropland reclamation in Northeast China, and significant warming was the main cause of the northward shift of FPE in region 1, especially after 2000 (Fig. 8c). During the 1980s–1990s, climate wetting in western Liaoning Province (SE-2) and the center of Inner Mongolia (NW-2) (Fig. 8h) accelerated the reclamation of cropland and extended the boundary of FPE in region 2.

In addition, human activity is another key factor that affects FPE shift in northern China. For example, the Grain for Green Project is the largest ecological restoration project ever implemented in a developing country to convert previously cultivated land to perennial non-native vegetation since 1999. The cropland area decreased in NW-2 and NW-3 due to this project, consequently the FPE was narrower in these regions during the 1990s–2000s (Fig. 8c and l). In addition, although the climate became wetter after 2000 on the Loess Plateau in SE-3, the cropland area decreased as the FPE shifted southward due to the Grain for Green Project in China (Fig. 8l).

4. Discussion

4.1. Comparisons of different proposed FPE shifts in northern China

Liu et al. (2011) divided the FPE into three sections and found that the boundary changes in the northeastern and northern sections were greater than those in the northwestern section. This result is in accordance with our findings, as the average ranges of gravity center shifts during the three periods decreased from northeast to southwest. The northeast section displayed the most obvious boundary shift, which was mainly because of climate warming. This conclusion was also observed by Ye and Fang (2012), who concluded that cropland expansion resulted in primarily northwestward FPE boundary shifts from 1980 to 2000 in the eastern FPE of northern China.

Most of the previous assessments of climate-induced ecotone shifts revealed the degree of fluctuation in response to historical climate change, and the FPE was often discussed as an entire region. Hence, research regarding the contributions of climate change to boundary shifts has been relatively limited. Some studies have documented the qualitative relationship between climate change and boundary shifts. Lu and Jia (2013) concluded that the FPE was closely related to fluctuations in precipitation associated with the East Asia monsoon climate from 1981 to 2005. Additionally, Liu et al. (2011) found that agricultural production activities did not change based on climatic change, and opposing variations in climatic and land use boundaries were observed in the late 20th century. This observation may the result of land use policies. By contrast, our findings show that FPE boundaries in

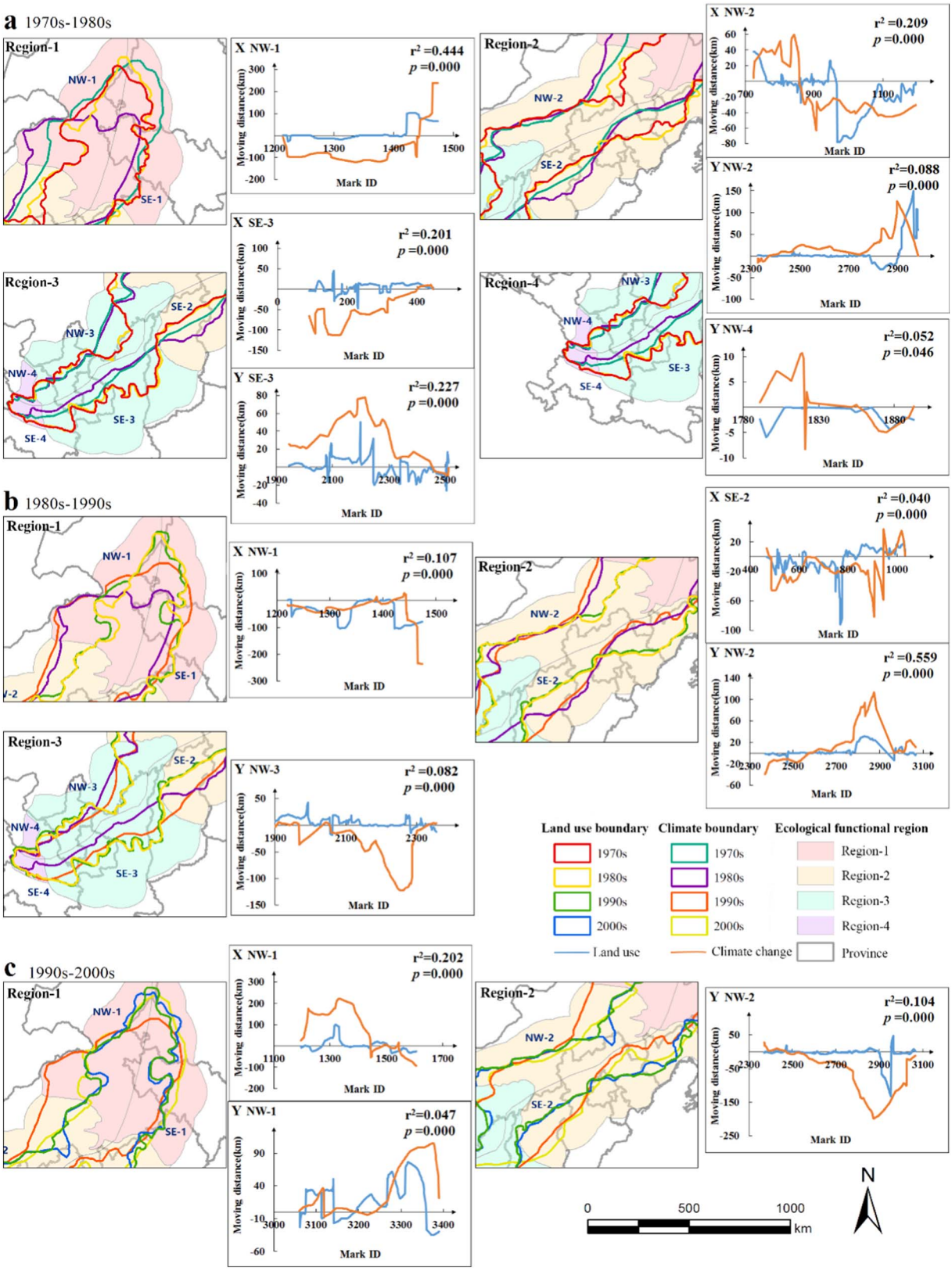

Fig. 6. The climate contributions to FPE boundary shifts detected in the X- and Y-coordinate directions in each ecological functional region of northern China during the (a) 1970s–1980s, (b) 1980s–1990s and (c) 1990s–2000s.

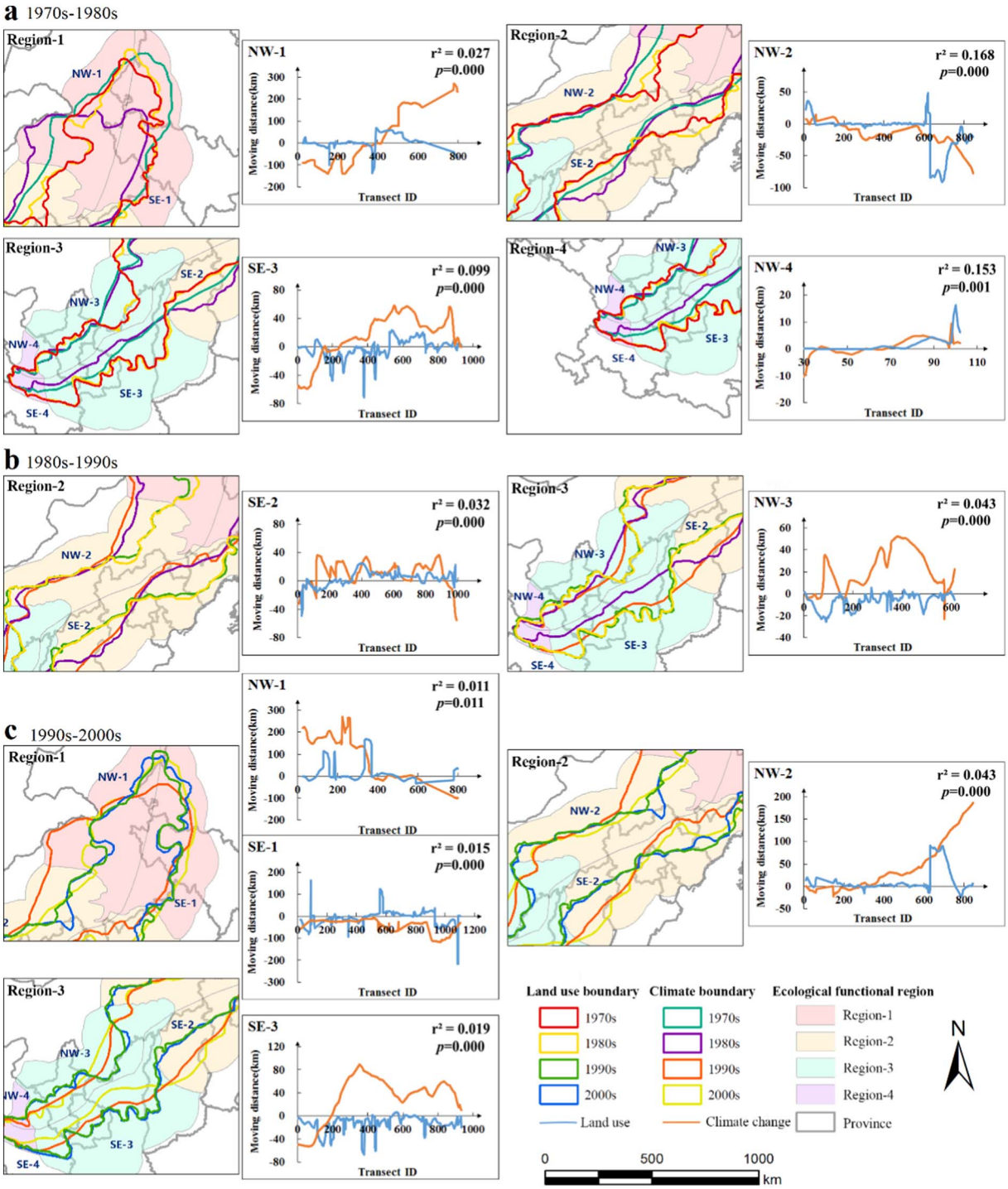

Fig. 7. The climate contributions to the FPE boundary shifts detected in the directions of transects along the boundaries of each ecological functional region in northern China during the (a) 1970s–1980s, (b) 1980s–1990s and (c) 1990s–2000s.

different spatial regions had different responses to climate change.

4.2. The comparison of results from different methods in the analysis framework

The method at line level to detect the boundary shifts in the X- and Y-coordinate directions can be easily applied in statistical analysis, and it can be conducted rapidly and directly at a large scale (Shi et al., 2017). However, it only can distinctly provide the boundary shifts based on the climate and land use data in the X- and Y- coordinate directions, which was not as accurate as the method to detect the boundary shifts in the directions of transects along the boundaries. Therefore, the method to detect boundary shifts in the transect direction is more suitable to be used in the situation of higher accuracy needed in the detection of the boundary shifts (Shi et al., 2017).

In addition, we also compared the results from the methods at point level, line level and area level. The boundary shifts detected by the methods at point and line levels concluded similar results. For the climate boundary, results from different methods showed that the largest and the smallest shifts were observed in regions 1 and 4, respectively. The boundary shifts moved southward in region 1, NW-3 and SE-2 during the 1970s–1980s, and then moved northward during the last

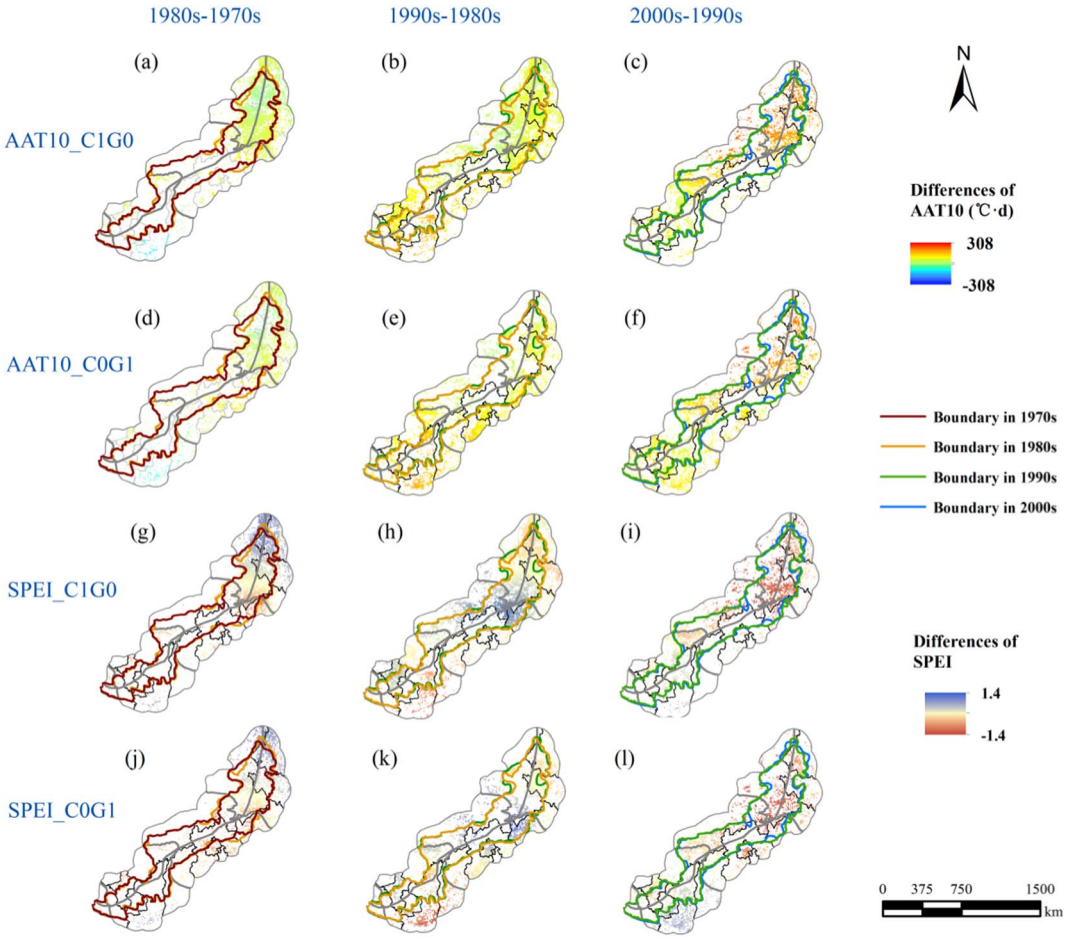

Fig. 8. The spatial analysis of land use change in response to climate change in the FPE of northern China. C1G0, cropland increase and grassland decrease; C0G1, cropland decrease and grassland increase.

two periods. Land use boundary moved southward in most of regions during the 1970s–1980s, and then moved westward during the 1980s–1990s. All the methods used to detect the relationships between climate and land use boundaries described that significant correlation existed in region 1, NW-2, NW-3 and SE-2 especially during the 1970s–1980s. The driving force analysis at area level has also proved the results of boundary shifts relationship and climate contributions at line level.

4.3. Study limitations

Intense climate variability and complicated anthropogenic activities made the actual FPE boundaries vary frequently each year; thus, the relationship between climate change and FPE boundary shifts is difficult to investigate. In addition, the FPE boundary shifts were measured based on the averaged locations of FPE boundaries during each period. Therefore, our research is a preliminary attempt to explore the contributions of climate change to boundary shifts quantitatively. Detailed variations in FPE boundaries could potentially be explored through further analysis of the inter-year variability in climate, farmer decisions, and other factors. In addition to climate change, other natural factors, such as edaphic factors, slope, altitude and human-induced land use changes, can affect crop cultivation (Feeley and Rehm, 2015; Liang et al., 2016; Pricope et al., 2013; Silva, 2014).

5. Conclusions

This paper focused on understanding the spatially explicit contributions of climate change to FPE boundaries in northern China. The FPE in northern China is ecologically fragile and geologically unstable, the boundary of which fluctuates at different periods due to both climate change and human factors. Based on detailed calculations at a grid scale of 1 km, we provided spatially explicit evidence of the effects of climate change on ecotone shifts. Compared with changes in climate boundaries, changes in land use boundaries were narrower, indicating that a lag effect exists between the boundaries of land use and climate. In addition, the land use boundaries were more fragmented than climate boundaries, further indicating that land use boundaries were mainly influenced by anthropogenic disturbances.

Significant differences in the climate contributions to FPE boundary shifts in different ecological regions of northern China were observed in the three study periods. In general, the contributions in regions 1 and 2 were more significant than other regions, further indicating that other factors, such as the Grain for Green Project, might be responsible for the observed land use change in the northwest China after 2000. Moreover, the southeastern part of FPE was influenced by human activities more than the northwestern one, and climate change contributed to the FPE boundary shifts less significantly in most regions in the southeast during the three periods. We suggest that specific mitigation and adaptation strategies be implemented in different regions and periods. Such strategies can be used to integrate food security and vulnerability associated with climate change into future decision making.

Acknowledgments

We thank Prof. Richard Strange for manuscript improvement, and the two anonymous reviewers for their useful comments on an earlier version of this manuscript. This study was supported by the National

Natural Science Foundation of China (Grant No. 41771111 and 41401113), Fund for Excellent Young Talents in Institute of Geographic Sciences and Natural Resources Research, Chinese Academy of Sciences (2106RC201), the National Natural Science Foundation of China (Grant No. 41430861 and 41471091), the Key Laboratory of Carrying Capacity Assessment for Resource and Environment, Ministry of Land and Resources (CCA2017.02), and the China Scholarship Council.

References

Adnan, F.A., Hamylton, S.M., Woodroffe, C.D., 2016. A comparison of shoreline changes estimated using the base of beach and edge of vegetation line at north Keeling Island. J. Coast. Res. 75 (sp1), 967–971.

Allen, C.D., Breshears, D.D., 1998. Drought-induced shift of a forest-woodland ecotone: rapid landscape response to climate variation. Proc. Natl. Acad. Sci. U. S. A. 95 (25), 14839–14842.

Berner, L.T., Beck, P.S., Bunn, A.G., Goetz, S.J., 2013. Plant response to climate change along the forest-tundra ecotone in northeastern Siberia. Glob. Chang. Biol. 19 (11), 3449–3462.

Blanco, C.C., Scheiter, S., Sosinski, E., Fidelis, A., Anand, M., Pillar, V.D., 2014. Feedbacks between vegetation and disturbance processes promote long-term persistence of forest-grassland mosaics in south Brazil. Ecol. Model. 291, 224–232.

Chen, C., Huang, D., Wang, K., 2015. Risk assessment and invasion characteristics of alien plants in and around the agro-pastoral ecotone of northern China. Hum. Ecol. Risk. Assess. 21 (7), 1766–1781.

Ebdon, D., 1985. Statistics in Geography. Blackwell, Oxford.

Fang, X., Ye, Y., Zeng, Z., 2007. Extreme climate events, migration for cultivation and policies: a case study in the early Qing Dynasty of China. Sci China Ser D-Earth Sci 50 (3), 411–421.

Feeley, K.J., Rehm, E.M., 2015. Downward shift of montane grasslands exemplifies the dual threat of human disturbances to cloud forest biodiversity. Proc. Natl. Acad. Sci. U. S. A. 112 (45), 6084.

Fernández, M., Hamilton, H.H., Kueppers, L.M., 2015. Back to the future: using historical climate variation to project near-term shifts in habitat suitable for coast redwood. Glob. Chang. Biol. 21 (11), 4141–4152.

Fu, B., Qi, Y., Chang, Q., 2015. Impacts of revegetation management modes on soil properties and vegetation ecological restoration in degraded sandy grassland in farming-pastoral ecotone. Int J Agr. Biol. Eng. 8 (1), 26–34.

Fu, C., 1992. Transitional climate zones and biome boundaries: A case study from China. In: Hansen, A.J., Di Castri, F. (Eds.), Landscape Boundaries: Consequences for Biotic Diversity and Ecological Flows. Springer-Velag, New York, pp. 394–402.

Ge, Q., Hua, Z., Zheng, J., Fang, X., Xiao, L., Liu, J., Yang, B., 2015. Forcing and impacts of warm periods in the past 2000 years (in Chinese). Chin. Sci. Bull. 60 (18), 1727–1734.

Ge, Q., Liu, H., Zheng, J., Xiao, L., 2013. The climate change and social development over the last two millennia in China (in Chinese). Chinese J Nat 35 (1), 9–21.

Gyasi, E., Agyepong, G., Ardayfio-Schandorf, E., Enu-Kwesi, L., Nabila, J., Owusu-Bennoah, E., 1995. Production pressure and environmental change in the forest-savanna zone of southern Ghana. Glob. Environ. Chang. 5 (4), 355–366.

Han, M., 2000. On the accommodation between human and environment during the last 2000 years and scientific inspiration (in Chinese). Geogr. Res. 19 (3), 324–331.

Hansen, A.J., Di Castri, F., Naiman, R.J., 1988. Ecotones: what and why? In: Di Castri, F., Hansen, A.J., Holland, M.M. (Eds.), A New Look at Ecotones: Emerging International Projects on Landscape Boundaries. Biology International, Special Issue 17. International Union of Biological Sciences, Paris, pp. 9–46.

Hart, J.F., 1954. Central tendency in areal distributions. Econ. Geogr. 30 (1), 48–59.

Huang, Q., Xin, X., Zhang, H., 2010. Ecosystem service based regionalization of the grassland and agro-pastoral transitional zone in nortnern China (in Chinese). Acta Ecol. Sin. 30 (2), 350–356.

IPCC, 2013. Summary for policymakers. In: Stocker, T.F., Qin, D., Plattner, G.-K., Tignor, M., Allen, S.K., Boschung, J., Nauels, A., Xia, Y., Bex, V., Midgley, P.M. (Eds.), Climate Change 2013: The Physical Science Basis. Contribution of Working Group I to the Fifth Assessment Report of the Intergovernmental Panel on Climate Change. Cambridge University Press, Cambridge, United Kingdom and New York, NY, USA.

Jayson-Quashigah, P.-N., Addo, K.A., Kodzo, K.S., 2013. Medium resolution satellite imagery as a tool for monitoring shoreline change. Case study of the Eastern coast of Ghana. J. Coast. Res. 65 (sp1), 511–516.

Kallepalli, A., Kakani, N.R., James, D.B., Richardson, M.A., 2017. Digital shoreline analysis system-based change detection along the highly eroding Krishna–Godavari delta front. J. Appl. Remote. Sens. 11 (3), 036018.

Kitzberger, T., 2012. Ecotones as complex arenas of disturbance, climate, and human impacts: The trans-Andean forest-steppe ecotone of northern Patagonia. In: Myster, R. (Ed.), Ecotones between Forest and Grassland. Springer, New York, pp. 59–88.

Li, Z., Yan, Z., 2009. Homogenized daily mean/maximum/minimum temperature series for China from 1960–2008. Atmos Oceanic Sci. Lett. 2 (4), 237–243.

Liang, E., Wang, Y., Piao, S., Lu, X., Camarero, J.J., Zhu, H., Zhu, L., Ellison, A.M., Ciais, P., Peñuelas, J., 2016. Species interactions slow warming-induced upward shifts of treelines on the Tibetan Plateau. Proc. Natl. Acad. Sci. U. S. A. 113 (16), 4380–4385.

Liu, J., Gao, J., Lv, S., Han, Y., Nie, Y., 2011. Shifting farming-pastoral ecotone in China under climate and land use changes. J. Arid Environ. 75 (3), 298–308.

Liu, J., Liu, M., Tian, H., Zhuang, D., Zhang, Z., Zhang, W., Tang, X., Deng, X., 2005. Spatial and temporal patterns of China's cropland during 1990–2000: an analysis based on Landsat TM data. Remote Sens. Environ. 98 (4), 442–456.

Liu, J., Liu, M., Zhuang, D., Zhang, Z., Deng, X., 2003. Study on spatial pattern of land-use change in China during 1995–2000. Sci China Ser D - Earth Sci. 46 (4), 373–384.

Liu, J., Zhang, Z., Xu, X., Kuang, W., Zhou, W., Zhang, S., Li, R., Yan, C., Yu, D., Wu, S., Jiang, N., 2010. Spatial patterns and driving forces of land use change in China during the early 21st century. J. Geogr. Sci. 20 (4), 483–494.

Lobell, D.B., Asner, G.P., 2003. Climate and management contributions to recent trends in US agricultural yields. Science 299 (5609), 1032.

Lu, W., Jia, G., 2013. Fluctuation of farming-pastoral ecotone in association with changing East Asia monsoon climate. Clim. Chang. 119 (3), 747–760.

Pricope, N.G., Husak, G., Lopez-Carr, D., Funk, C., Michaelsen, J., 2013. The climate-population nexus in the East African Horn: Emerging degradation trends in rangeland and pastoral livelihood zones. Global Environ. Change-Human Pol. Dimens. 23 (6), 1525–1541.

Scheffer, M., Hirota, M., Holmgren, M., Van Nes, E.H., Chapin, F.S., 2012. Thresholds for boreal biome transitions. Proc. Natl. Acad. Sci. U. S. A. 109 (52), 21384–21389.

Sharma, L.N., Vetaas, O.R., Chaudhary, R.P., Måren, I.E., 2014. Ecological consequences of land use change: Forest structure and regeneration across the forest-grassland ecotone in mountain pastures in Nepal. J. Mt. Sci. 11 (4), 838–849.

Shi, W., Liu, Y., Shi, X., 2017. Development of quantitative methods for detecting climate contributions to boundary shifts in farming-pastoral ecotone of northern China. J. Geogr. Sci. 27 (9), 1059–1071.

Shi, W., Tao, F., Liu, J., Xu, X., Kuang, W., Dong, J., Shi, X., 2014. Has climate change driven spatio-temporal changes of cropland in northern China since the 1970s? Clim. Chang. 124 (1–2), 163–177.

Silva, L.C., 2014. Importance of climate-driven forest-savanna biome shifts in anthropological and ecological research. Proc. Natl. Acad. Sci. U. S. A. 111 (37), 3831–3832.

Staver, A.C., Archibald, S., Levin, S.A., 2011. The global extent and determinants of savanna and forest as alternative biome states. Science 334 (6035), 230.

Thieler, E.R., Himmelstoss, E.A., Zichichi, J.L., Ergul, A., 2009. Digital Shoreline Analysis System (DSAS) version 4.0-An ArcGIS extension for calculating shoreline change. In: US Geological Survey Open-File Report 2008–1278 *current version 4.3..

Van Vliet, N., Mertz, O., Heinimann, A., Langanke, T., Pascual, U., Schmook, B., Adams, C., Schmidt-Vogt, D., Messerli, P., Leisz, S., 2012. Trends, drivers and impacts of changes in swidden cultivation in tropical forest-agriculture frontiers: a global assessment. Global Environ. Change-Human Pol. Dimens. 22 (2), 418–429.

Wang, J., Shi, P., 1988. The utilization of land resources and regional development strategies of farming-pastoral zone in Inner Mongilia (in Chinese). Areal Res. Dev. 7 (1), 24–28.

Wang, Z., Jiang, J., Liao, Y., Deng, L., 2015. Risk assessment of maize drought hazard in the middle region of farming-pastoral ecotone in Northern China. Nat. Hazards 76 (3), 1515–1534.

Wasson, K., Woolfolk, A., Fresquez, C., 2013. Ecotones as indicators of changing environmental conditions: rapid migration of salt marsh-upland boundaries. Estuar. Coasts 36 (3), 654–664.

Williams, A.P., Allen, C.D., Macalady, A.K., Griffin, D., Woodhouse, C.A., Meko, D.M., Swetnam, T.W., Rauscher, S.A., Seager, R., Grissino-Mayer, H.D., Dean, J.S., Cook, E.R., Gangodagamage, C., Cai, M., McDowell, N.G., 2013. Temperature as a potent driver of regional forest drought stress and tree mortality. Nat. Clim. Chang. 3 (3), 292–297.

Wu, C., Guo, H., 1994. The Land Use of China (in Chinese). Science Press, Beijing.

Wu, F., Zhan, J., Yan, H., Shi, C., Huang, J., 2013. Land cover mapping based on multisource spatial data mining approach for climate simulation: a case study in the farming-pastoral ecotone of north China. Adv. Meteorol. 2013, 1–12.

Ye, Y., Fang, X., 2012. Expansion of cropland area and formation of the eastern farming-pastoral ecotone in northern China during the twentieth century. Reg. Environ. Chang. 12 (4), 923–934.

Ye, Y., Fang, X., Khan, M.A.U., 2012. Migration and reclamation in northeast China in response to climatic disasters in north China over the past 300 years. Reg. Environ. Chang. 12 (1), 193–206.

Ye, Y., Fang, X., Ren, Y., Zhang, X., Chen, L., 2009. Cropland cover change in northeast China during the past 300 years. Sci China Ser D-Earth Sci 52 (8), 1172–1182.

Yu, L., Zhang, S., Liu, T., Tang, J., Bu, K., Yang, J., 2014. Spatio-temporal pattern and spatial heterogeneity of ecotones based on land use types of southeastern Da Hinggan Mountains in China. Chin. Geogr. Sci. 25 (2), 184–197.

Zhang, Z., Zhao, X., Wang, X., 2012. Remote Sensing Monitoring of Land Use in China (in Chinese). Star Map Press, Beijing.

Zuo, L., Zhang, Z., Zhao, X., Wang, X., Wu, W., Yi, L., Liu, F., 2014. Multitemporal analysis of cropland transition in a climate-sensitive area: a case study of the arid and semiarid region of northwest China. Reg. Environ. Chang. 14 (1), 75–89.